

Recursive symmetries for geometrically complex and materially heterogeneous additive manufacturing



Christoph Bader, Neri Oxman*

Mediated Matter Group, Media Lab, Massachusetts Institute of Technology, Cambridge, MA 02139, USA

ARTICLE INFO

Article history:

Received 6 July 2016

Accepted 12 September 2016

Keywords:

Generative design

Additive manufacturing

Mass-customization

Multi-material 3D-printing

Design-exploration

ABSTRACT

We present a generative method for the creation of geometrically complex and materially heterogeneous objects. By combining generative design and additive manufacturing, we demonstrate a unique form-finding approach and method for multi-material 3D printing. The method offers a fast, automated and controllable way to explore an expressive set of symmetrical, complex and colored objects, which makes it a useful tool for design exploration and prototyping. We describe a recursive grammar for the generation of solid boundary surface models suitable for a variety of design domains. We demonstrate the generation and digital fabrication of watertight 2-manifold polygonal meshes, with feature-aligned topology that can be produced on a wide variety of 3D printers, as well as post-processed with traditional 3D modeling tools. To date, objects with intricate spatial patterns and complex heterogeneous material compositions generated by this method can only be produced through 3D printing.

© 2016 Elsevier Ltd. All rights reserved.

1. Introduction

Symmetries are abundant in the domains of mathematics, the sciences and the arts [1]. Throughout history, and across scales of material practice – within architecture, arts and crafts – symmetries can be found in combination with color, as can be observed in fabricated ornamental artifacts known to carry and express cultural identity and significance [2]. Within the natural world alone, a multitude of symmetrical forms are thought to have evolved as a consequence of the need to identify and to recognize objects [3]. Furthermore, symmetries are known to be associated with genetic quality [4] and, along with complexity, symmetries have long been associated with the perception of beauty [5].

While known to enable the creation of highly complex objects [6], the availability of generative design methods that enable the creation of objects that are *truly complex* – both in shape and in material composition – is limited. Furthermore, implemented rule-sets are often restricted to the generation of *specific* types of artifacts. As such, the resulting objects are generally not diverse. And, even when they do enable geometrical diversity, such generative methods often generate descriptions that are not directly suitable for 3D printing or yet do not produce material distributions alongside geometry. Thus, generative design methods are typically not

used in combination with streamlined workflows supporting the generation of physical material distributions for multi-material 3D printing.

Driven by the motivation to overcome such limits, and by design opportunities associated with them, we present a generative method that enables the creation of a diverse set of geometrically complex colored objects, driven by symmetry.

The presented method can generate a wide variety of 3D printable objects with geometry-associated material distributions, and – as a result – it can be utilized as a valuable tool for the customizable generation of geometrically and materially complex 3D printable artifacts for use in creative workflows, design-exploration and the generation of unique 3D printable objects.

Generative methods are well known in research areas associated with generative design [7]. They embody process descriptions and rule-based systems for the semi-autonomous generation of artifacts such as images, sounds, animations, or 3 dimensional objects. These descriptions act in a similar way to DNA, in the biological world. The generative method is either controlled by parameters or by making direct modifications to the algorithm itself. One usually distinguishes between the algorithm or process created by the generative designer, the parameter controlled instance of the process utilized by the method's designer (or a third person), and the artifacts generated by that instance. Recently, generative methods have been utilized as mass-customization tools with 3D printing being a means for production to give users the opportunity to generate unique

* Correspondence to: MIT Media Lab, 75 Amherst Street, E14-433C, Cambridge, MA 02139, USA.

E-mail address: neri@mit.edu (N. Oxman).

objects. Examples include Cell Cycle by Nervous Systems [8] and Autodesk's Shapeshifter [9]. As generative methods enable the generation of complex geometries by automation and customization by parameterization, 3D printing has become the only viable method that enables the transformation of arbitrary generated output into physical form, without losing the benefits of the generative method [10].

Multi-material 3D printing [11] enables the additive fabrication of objects comprised of multiple materials heterogeneously distributed within a single build, omitting the need for assemblies. In this paper we present 3D models that have been digitally fabricated by depositing UV-curable resin droplets in an inkjet like fashion, layer-by-layer. Every new layer of jetted ink is cured through UV-light while nearby droplets diffuse and aggregate with the surrounding deposited droplets, and through successive repetition, form a 3D volume. Recently, developed methods for heterogeneous material distributions have found their application as a tool for design expressions, most prominently featured in the work of Neri Oxman and the Mediated Matter Group [12].

In the following section we present a method for the generation of customizable and highly articulated objects; we showcase a diversity of outcomes, we evaluate the method's usefulness; and, finally, we describe the digital fabrication process of the generated objects through multi-material 3D printing.

2. Method

2.1. Description

The method implemented defines a recursive parametric grammar using polyhedral forms. Polyhedra are initially represented as polygonal meshes that, iteratively, 'evolve' into subdivision surfaces in a process resembling cellular division. This is achieved through the application of a recursive rule transforming the polygonal mesh, consisting of a collection of vertices, edges and faces, that will subsequently be used as the "control mesh" for the generation of a subdivision surface. This method, and its formalism, resembles shape-grammar formalisms [13]. Grammar-based formalisms have been successfully utilized in a wide variety of design settings [14], especially in the design of patterns mimicking cultural artifacts [15]. Similarly, our method defines a grammar in the vein of boundary solid grammars [16], using only a limited set of rules while offering a high level of diversity of shapes.

We define Ω as the mirroring of a polygonal mesh along a given plane. Here mirroring refers to Ω cutting a polygonal mesh by a given plane, discarding regions in the negative half-space of the plane, subsequently reflecting the resulting mesh across this plane and obtaining a boolean union with the original non-reflected shape. Thus, given a set P of planes in \mathbb{R}^3 , $P = \{p_1, \dots, p_n\}$, we denote the operator Ω as a function taking a coarse polygonal mesh M^0 with possible vertex or face properties. Here, M^i is a mesh with vertices $V_M = \{v_1, \dots, v_n\}$ and faces $F_M = \{f_1, \dots, f_m\}$, $f_j \in V_M \times \dots \times V_M$ where a position $p(v_i)$ in \mathbb{R}^3 is associated with each vertex $v_i \in V_M$. Besides position we assume that there is an additional property C , carrying ratios of material-distribution information, associated with each vertex or face such that $C = \{c_1, \dots, c_n\}$, $c : V_M \rightarrow C$, $c_i = c(v_i)$ or $C = \{c_1, \dots, c_n\}$, $c : F_M \rightarrow C$, $c_i = c(f_i)$ respectively. Ω takes M^0 and transforms it into a symmetrical mesh M^1 by sequentially cutting and mirroring it as follows

$$M^1 = \Omega_{p_1}(M^0) = \text{mirror}(\text{cut}(M^0, p_1), p_1).$$

Here the *cut* operation is the boolean intersection of M^i with the positive half-space defined by p_{i+1} resulting in an open mesh. The mirroring procedure produces a symmetrical mesh along p_1 and the resulting mesh must be closed. This can be

achieved by reflection of the original mesh and performing a boolean union with the original mesh. Finally we assume that Ω does not introduce degenerated non 2-manifold cases such as singular vertices or complex edges [17]. The operator is repeated recursively for n user-defined steps resulting in M^n .

$$M^i = \Omega_{p_i}(M^{i-1}).$$

The resulting mesh may have unconnected parts $N = \{M^{n_1}, M^{n_2}, \dots, M^{n_k}\}$, where $M^n = \bigcup M^{n_i}$ and $\forall M^{n_i}, M^{n_j} \in N$ with $i \neq j \Rightarrow M^{n_i} \cap M^{n_j} = \emptyset$. From these, we find the largest surface area and find $M_{\max} = \text{argmax Area}(N)$ where *Area* is the usual $\sum_{f \in F} n \cdot \sum_{v_i \in f} \frac{p(v_i) \times p(v_{i-1})}{2}$. We keep the largest part in order to obtain a connected mesh. Finally, M^{\max} is used as control polyhedron and recursively refined by the Catmull–Clark subdivision scheme [18] to obtain the final output M^f . We use the Catmull–Clark scheme as it results in M^f consisting of quadrilaterals and it enables the alignment of quadrilaterals with symmetries of the resulting object [19]. The method is depicted in Fig. 1, and exemplary outputs are shown in Figs. 2–4. We note that by adhering to the aforementioned conditions, M^f will be a closed 2-manifold polygonal mesh and, as such, it would be suitable for 3D printing. This process can be described in a grammar formalism, where the formal grammar G is given by $G = (\{M^i, |1 \leq i \leq n\}, M^f, \{\Omega_{p_i}, M^n \rightarrow M^{\max}, M^{\max} \rightarrow M^f\}, M^0, P)$.

2.2. Parameters, modification & evaluation

The appearance of the output M^f is typically governed by the input Mesh M^0 , and the number and configuration of the planes in the set P , given by plane normal $n_p(p_i)$ and distance $d_p(p_i)$ from the origin. Several generated examples are given in Fig. 2, showcasing various levels of heterogeneity in material composition. Fig. 3 illustrates the effect of different arrangements of planes on the outcomes. Planes must be defined such that they always pass through the currently largest object (given by the surface area). To achieve well-defined cutting, we precompute the largest part, before actually performing the cutting operation. Thus, planes which do not cut this largest part, can be adjusted accordingly during recursive execution of the process.

Interesting variations are achieved by incrementally increasing the distance from the origin for the planes in P such that $d_p(p_i) < d_p(p_j)$, for $i < j$. While random normal distributions for the planes P work well, aligning the plane-normals, as shown in Fig. 4 along a certain direction results in particular interesting examples.

Furthermore, we can increase the 'expressiveness' of the algorithm by modifying the *mirror* operation. By introducing deformations or geometric operations that are *distinct* for the two symmetrical sides generated, we can achieve an even greater diversity in the output. More generally reflections across arbitrary geometries are also possible as shown in Fig. 5(d). However, 'manifoldness' in this case is harder to achieve or must be sacrificed. To achieve reflections, we use a triangular mesh T instead of a plane across which the M should be reflected. To reflect we simply find the closest point k_i for the vertex $v_i \in V_M$ on T then compute the corresponding surface normal n_i at k_i and reflect across the plane defined by k_i and n_i . This is shown in Fig. 4. Manifoldness is sacrificed as this reflection mapping is no longer necessarily injective. If the reflection mapping can be given by a deformation mapping $F : \mathbb{R}^3 \rightarrow \mathbb{R}^3$ we must require that $\det(DF(p(v_i))) \neq 0$ for all $v_i \in V_M$ where DF denotes the Jacobian of F .

We note that, while the presented method appears simple, it produces outcomes that are otherwise challenging to reproduce, are sophisticated in detail and rich in complexity, and showcase

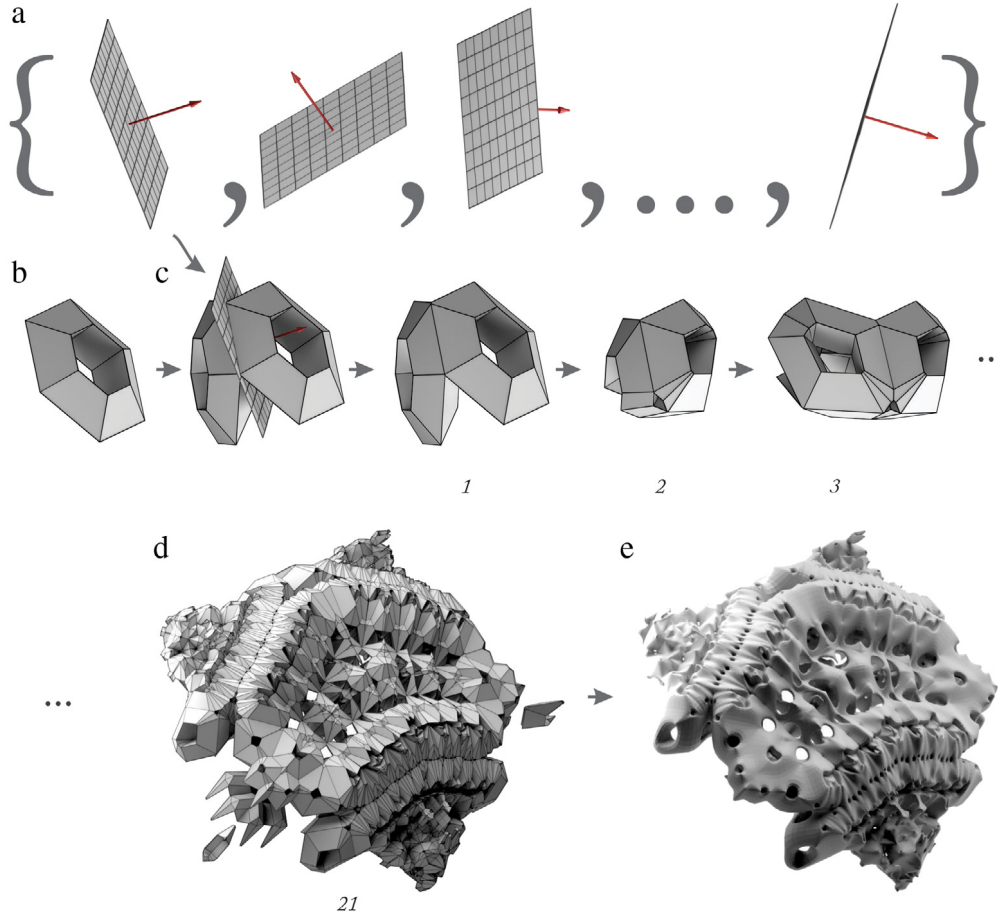


Fig. 1. A visual representation of the generative method. (a) a set of planes is generated as the base or underlying framework for all subsequent operations; (b) a user-guided input mesh is generated, upon which all operations are executed; (c) based on (b), a symmetrical mesh is generated; (d) the method is recursively re-applied and the result, following 21 iterations, is shown; (e) smaller sub-meshes are deleted and the subdivision surface is generated to produce the final artifact.

a high level of diversity. We also highlight the similarity of some of the produced artifacts to the artistic work of Nick Ervinck [20] or Michael Hansmeyer [21], who use 3D printing as a fabrication method, thereby showcasing the usability of the method for creative practice. Furthermore, as argued in [5], complex symmetrical patterns – as produced by our method – show a high correlation with aesthetic ‘judgments’ of beauty. As such, given the high diversity produced, and the ability to create objects that are considered “aesthetically pleasing”, the method is suitable for the exploration of artistic design possibilities and, thereby, can enhance or contribute to the creative process. Finally, the outcome’s feature-aligned topology allows for straightforward and efficient editing of the generated meshes with common 3D modeling tools.

Similarly to [22], we evaluate our method by performance, stability, expressivity, control and applicability. We argue that, since the method is based upon operations with low computational complexity, and given that all operations are efficiently implementable using a half-edge data structure [23]; adequate performance can be achieved such that models with millions of vertices can be generated in seconds. This is experimentally verified as shown in Fig. 5(a), where models up to one million polygons are generated within a single second. The method produces objects reliably as all sub-operations are well studied and do not produce degenerated cases easily. As such, the method can be qualified as stable. The expressivity of the method is shown in Figs. 1–3. We argue that the method can produce a wide variety of diverse and interesting shapes. To investigate this diversity further, we

show that generated objects can be drastically dissimilar. To evaluate dissimilarity, we utilize weighted spectral distances [24], a shape distance measure similar to the distance obtained from the well-known Shape-DNA [25]. For two given shapes $\Omega_\lambda, \Omega_\xi$ the weighted spectral distance (WESD) uses the spectra $\{\lambda\}_{n=1}^\infty, \{\xi\}_{n=1}^\infty$ of the Laplace–Beltrami operator to define the distance given by $\rho(\Omega_\lambda, \Omega_\xi) \triangleq \left[\sum_{n=1}^\infty \left(\frac{|\lambda_n - \xi_n|}{\lambda_n \xi_n} \right)^p \right]^{1/p}$. For dissimilarity measurements we consider a set of 10 generated meshes shown in Figure 9, using the same input mesh throughout, and compute their mutual WESD. For each generated mesh we compute the discrete Laplace–Beltrami operator by its finite element approximation [26]. Using a spectra signature size of 100, we evaluate the WESD with $p = 2$ between each object and apply classical MDS to visualize the results as shown in Fig. 5(b). The distribution of the generated samples in the MDS plot clearly shows dissimilarity of the exemplary generated objects. Furthermore, as Fig. 5(c) shows dissimilarity can be achieved between generated objects by simply varying parameters of the method.

Control over generated outcomes is the method’s single limiting factor. While the amount and configuration of planes, the input shape and additional modified mirror operations are possible, there is no target-specific control that allows a user to modify the shape of the resulting object locally without modifying the global shape. This, however, does not limit the explorative nature of the method. Choosing a fixed number of planes, and continuously varying plane normal, distance of each plane or other parameters (Fig. 5(c)), while not performing the recursive subdivision step, heuristic design optimization methods [27] can be employed to fit

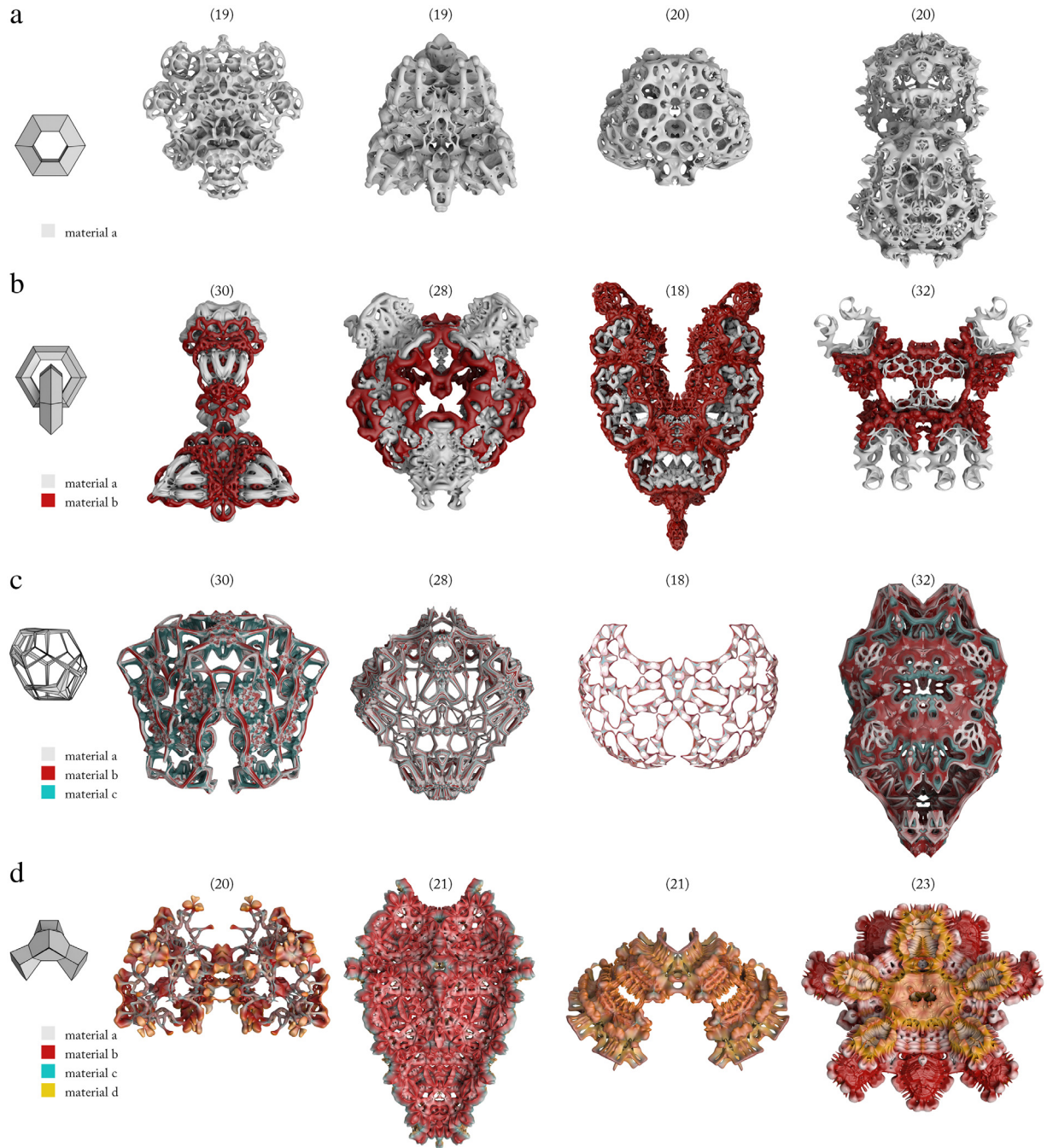


Fig. 2. Different input shapes and their results. Here the cardinality of the given plane-sets is shown in parentheses. In addition, we show different generated material distributions over the surface of the generated geometry with varying heterogeneity. (a) a single material, showcased by only one color; (b) two discretely disjoint geometries and materials; (c) geometrical discrete but materially heterogeneous material distributions; (d) geometrically heterogeneous and materially heterogeneous material distribution. Here we use color but as shown in Section 3 the colored material can encode for arbitrary printable materials and gradients between colors are visual indicators for intermediate mixed materials. (For interpretation of the references to color in this figure legend, the reader is referred to the web version of this article.)

the resulting object to a target envelope by minimizing the total Hausdorff distance between this target and the generated objects, as shown in Fig. 6. We discuss the applicability, of our method for the generation of 3D printable shapes in the next section.

3. Production

Since objects are generated without the direct influence of a user, it is important to validate that generated geometries are suitable for 3D printing. As described above, the objects generated by our method are inherently suitable for 3D printing, as outcomes

can be characterized, in most cases, as closed 2-manifold polygonal meshes separating an inner and an outer domain. We assume that the input mesh M_0 is a closed piecewise linear (PL) 2-manifold embedded in \mathbb{R}^3 . The cut operation removes regions of this surface which are in the negative half-plane given by p_i , leaving a PL 2-manifold embedded in \mathbb{R}^3 with boundary. The generated boundary is required to be a set of closed 1-manifolds embedded in \mathbb{R}^2 (closed curves). This is achieved by picking or adjusting the cutting planes such that – if a violating case is detected – the plane is slightly offset along its normal direction. This cut mesh is then reflected, and topologically connected, with its not reflected counterpart giving M_{i+1} . Thus, if the original shape M_0 is

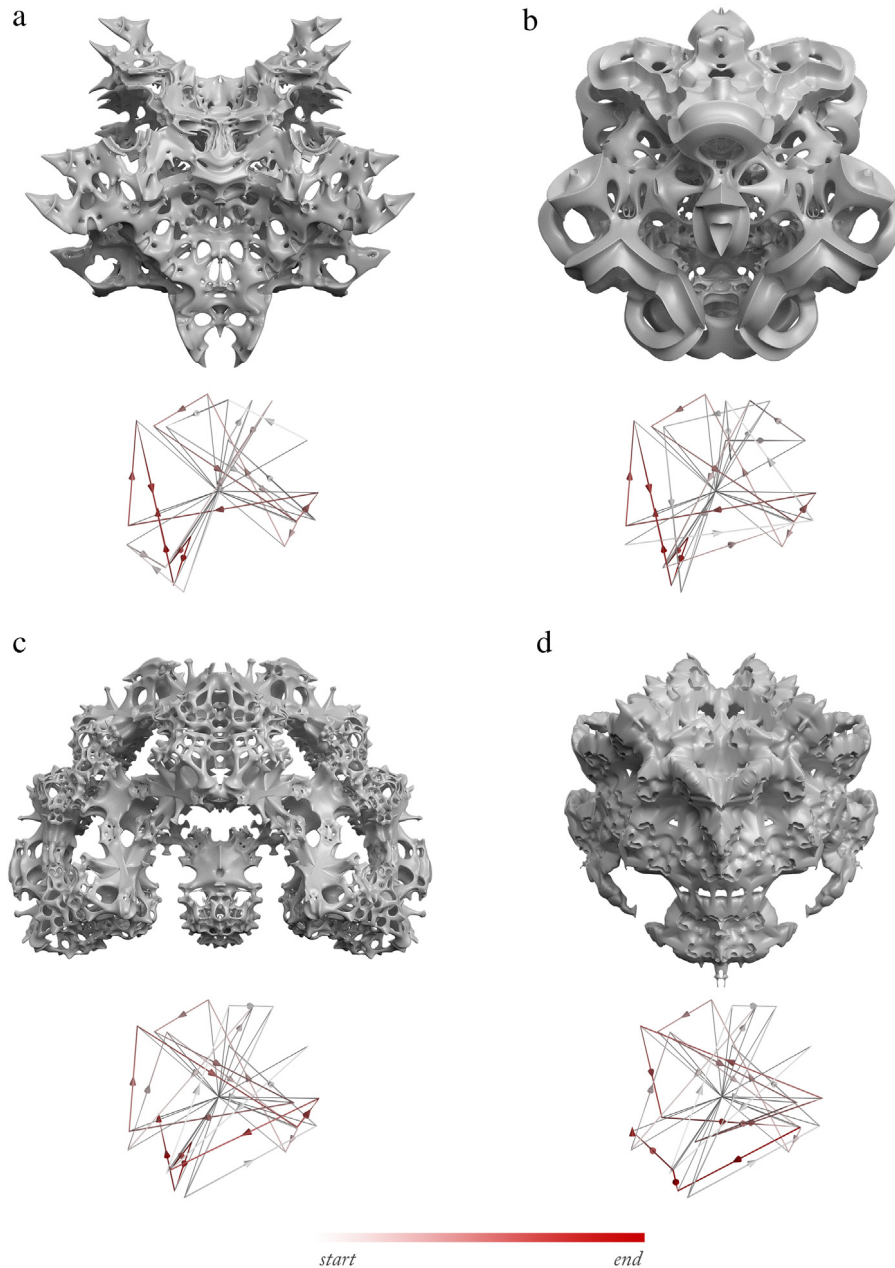


Fig. 3. All the generated objects utilize the same distribution of planes, but traverse them in different orders. Each section shows the generated object on top and the order in which the planes, depicted by their normal, are traversed below. (a) and (b) have different starting orders but the same order of planes in the end. (c) and (d) have the same starting order but diverge to different orders in the end.

a closed 2-manifold, at no point self-intersections or non-manifold cases such as singular vertices and complex edges are introduced. Furthermore, we require that, M^0 must only consist of convex polygons to avoid the introduction of overlapping polygons in the subdivision step. We also note that, while other approaches – such as the generation of 3D Mandelbrot-sets [28] – can result in similar shapes; these representations must be converted to a 3D printable format, typically by implementing iso-surfaces extraction methods [29], which can result in loss of surface-detail or large file-sizes.

Two case study models were fabricated on a Stratasys J750 multi-material 3D printer, capable of printing several photopolymer resins simultaneously. During print time, the print head simultaneously deposits resin droplets in various amounts that mix and immediately polymerize through exposure to UV light. By combining several types of base resins by spatial deposition, it is possi-

ble to achieve a wide variety of intermediate materials, which are rich in both color and structural properties. The standard workflow, available through the software interface to the 3D printer, uses predefined material combinations that can only be applied to individual disjoint model parts, which then have constant properties through the whole model part volume. While this workflow is sufficient for certain use cases, it is not applicable, nor is it ideal, for the production of parts resulting from our generative method. This is due to the fact that material properties are either encoded as vertex or face properties and can continuously vary across and between them. As such, we employ a custom slicing approach.

As shown in Fig. 7, we begin by generating a rasterized slice from M^f . Following, we determine the material properties from the surface, and, finally we 3D dither the slices to bitmaps, one for each of the base-materials being deposited by the printer. These dithered slices are used for the control of droplet placement by the

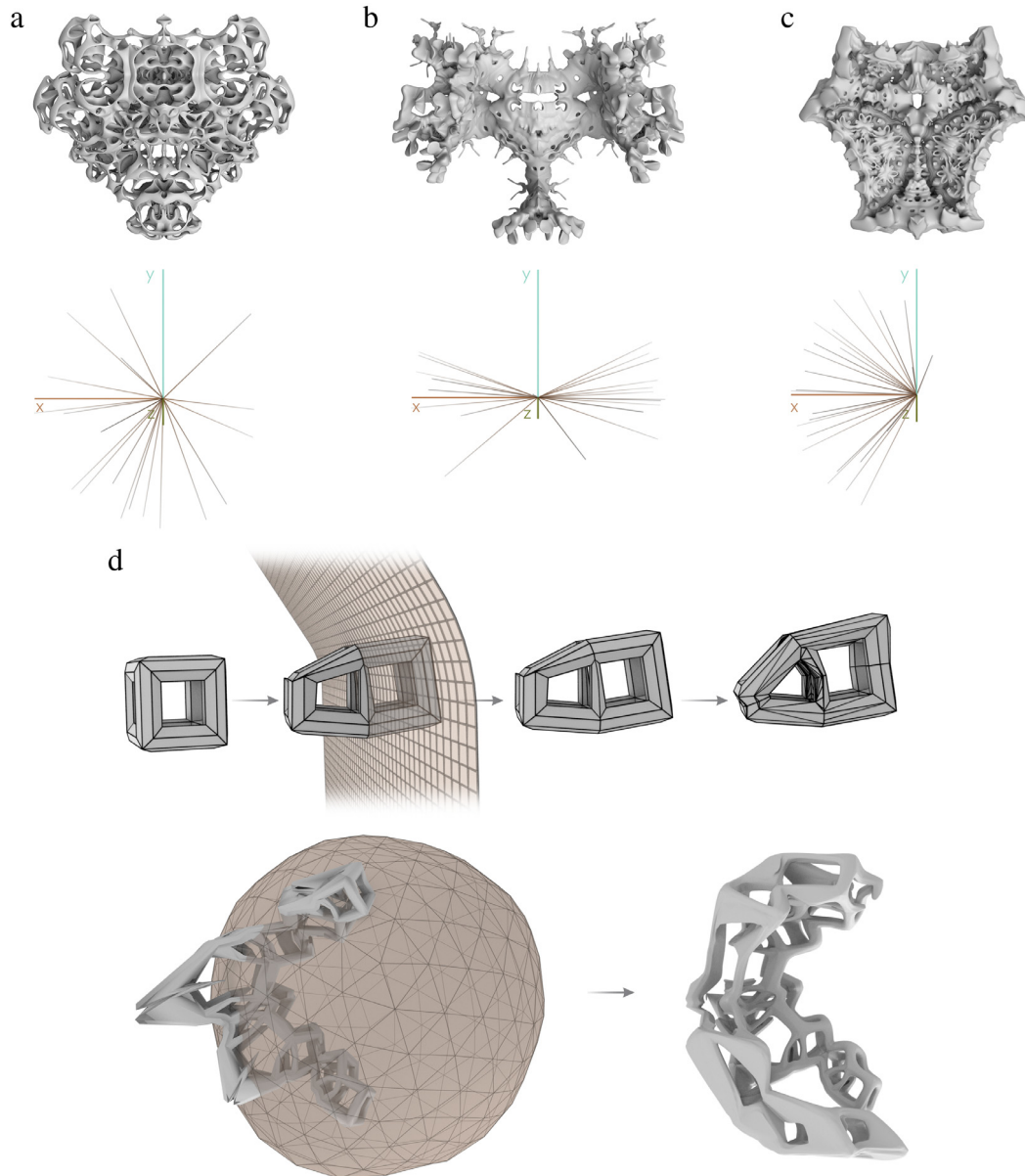


Fig. 4. Upper: Sets of plane-normals and respective outcomes. (a) a uniform distribution of plane normals; (b) plane normal distribution aligned with x -axis; (c) plane normal distribution aligned with positive x -axis only. Lower: (d) Reflection across arbitrary shapes such as deformed planes or spheres enabling more general outcomes.

printer, where near-by placed droplets will diffuse to aggregate into intermediate materials depending on the given spatial configuration and the types of materials being deposited [30,31]. Here we assume that $c_i \in C$ on M^f is an n -dimensional vector, where n is given by the number of base materials that the printer can provide, and, further, we require that $|c_i|_1 = 1$. In order to find – based on the properties of M^f – the internal material properties of the slice S_i , a new property C_{S_i} is associated with each voxel u_{ij} of the slice, such that: $u_{ij} \in S_i$, $C_{S_i} = \{c_{i1}, \dots, c_{in}\}$, $c_{S_i} : S_i \rightarrow C_{S_i}$, $c_{S_i} := c_{S_i}(u_{ij})$. We note that – while the property C_{S_i} can encode for color by describing the mixing ratios of Cyan, Magenta, Yellow, Black, White and Transparent resins – it can also encode for the mixing ratios of arbitrary resins with different functional properties, such as shore-hardness. In order to find the properties from the surface, we use an approach similar to inverse distance weighting. For each voxel u_{ij} in the slice S_i we sample the k closest points $K \subseteq V_M = \{v_1, \dots, v_n\}$ that are visible from u_{ij} , where $v_k \in K$ is visible from u_{ij} if the line segment from $p(v_k)$ to $p(u_{ij})$ lies in M . From the points in K we compute the new

property by

$$c_{S_i}(u_{ij}) = \frac{1}{\sum_{v_k \in K} (1 - \lambda(d(u_{ij}, v_k)))} \sum_{v_k \in K} (1 - \lambda(d(u_{ij}, v_k))) c(v_k)$$

where λ is a smoothing function for example given $\lambda(d) = 6 \left(\frac{d}{d_{\max}}\right)^5 - 15 \left(\frac{d}{d_{\max}}\right)^4 + 10 \left(\frac{d}{d_{\max}}\right)^3$, $d_{\max} = \max(d(u_{ij}, v_k))$ for all $v_k \in K$ and d is the Euclidean distance. If M is coarse, additional sample points, V_S , can be generated on the surface M and $V_M \cup V_S$ can be used to find the closest points, $K \subseteq V_M \cup V_S$. Following, for any additional $v_k \in V_S$, we compute $c(v_k)$ on M implementing barycentric interpolation from the vertices adjacent to the triangle on which v_k resides. An analogous approach can be used for properties associated with faces.

Furthermore, to each vertex $v_k \in V_M$ we can assign a maximum distance $\max d(v_k)$. We can then modify the set K such that for every v_k , this applies: $v_k \in K$, $d(u_{ij}, v_k) \leq \max d(v_k)$. This allows to constrain the influence region of each vertex within

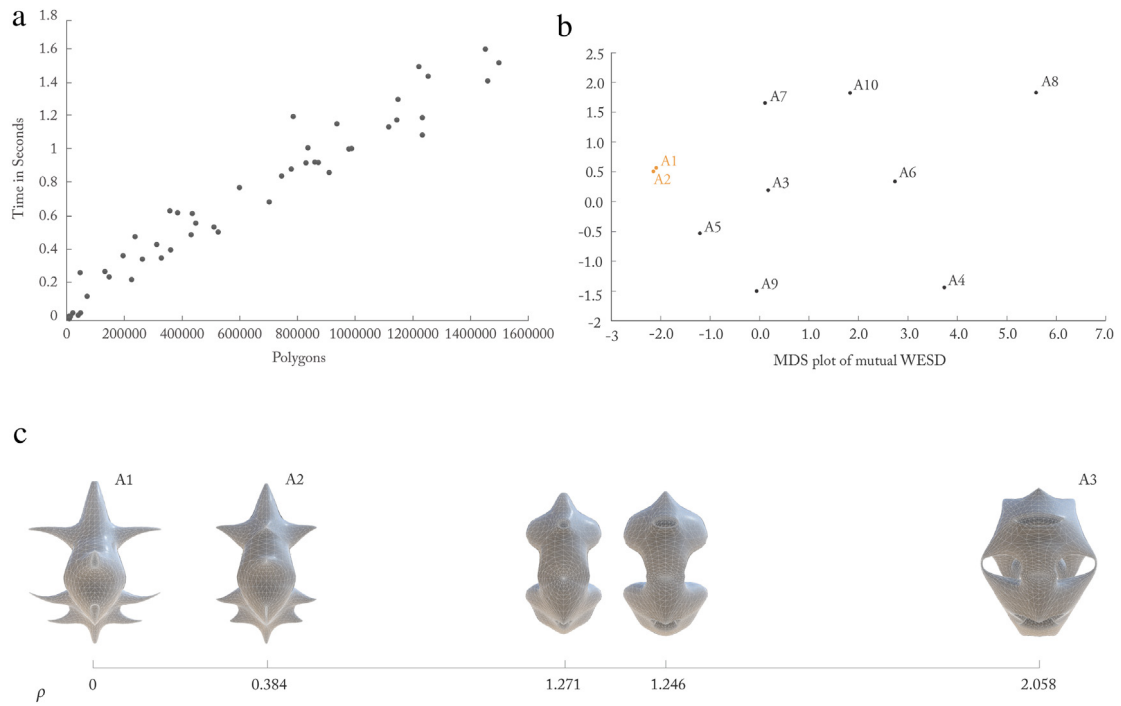


Fig. 5. (a) Performance measurements of the method for generated models with different polygon counts. All measurements were taken on an Intel Xeon E5-1650v3 with 3.50 GHz. (b) MDS-plot of weighted spectral distances. While the objects A1 and A2 were intentionally generated to be similar, objects A3–A10 have been generated with arbitrary parameters but from the same input mesh. (c) By continuously modifying the alignment of the input geometry the generated geometry changes, which results in a monotonically increasing WESD. In the evaluated objects we were limited to objects with low complexity (Polygon counts below 10 000) due to the high computational overhead for computing the spectra. All evaluate shapes are shown in supplemental figure 9.

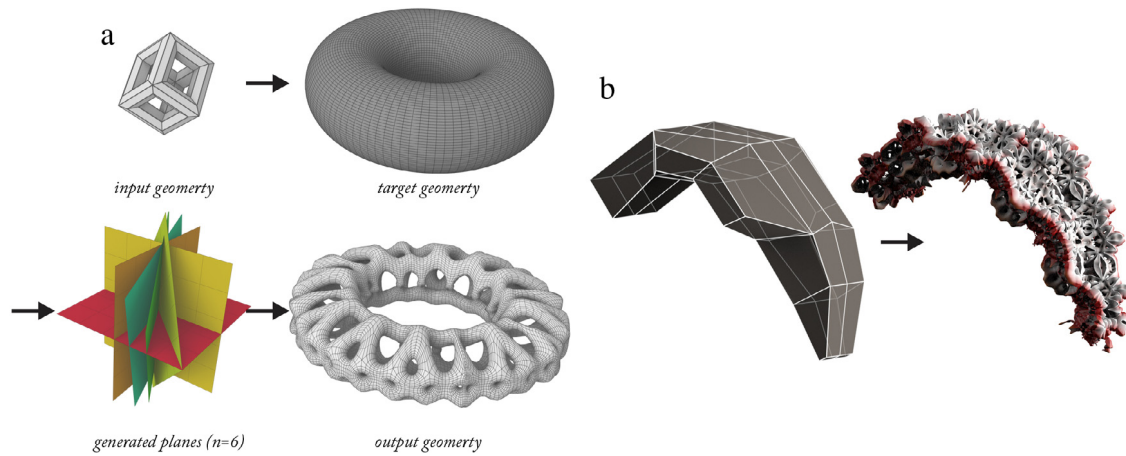


Fig. 6. Adapting a generated shape to a given target geometry. (a) The input geometry is to be transformed such that – following several applications of Ω – it fits to target geometry. To achieve this, the mirroring planes, must be determined as shown. Illustration (b) shows a more complex envelope shape with more complex internal shape.

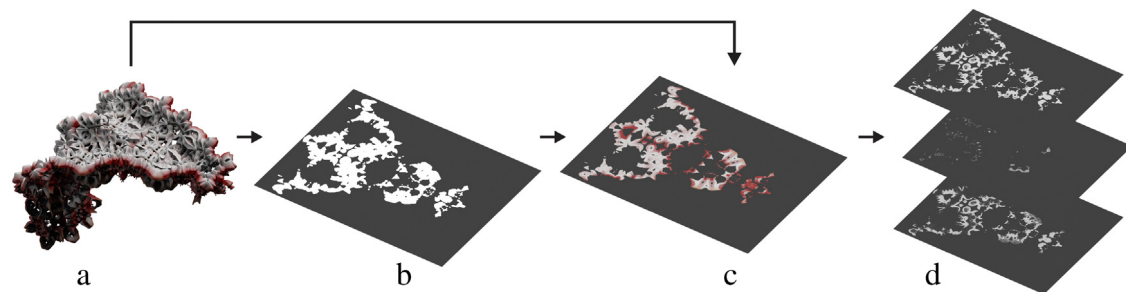


Fig. 7. The slicing process. (a) the input mesh; (b) the generated and rasterized slice; (c) contributing material information on the mesh is found per slice; (d) dithering to 3 bitmaps describing droplet placement of three base resins.

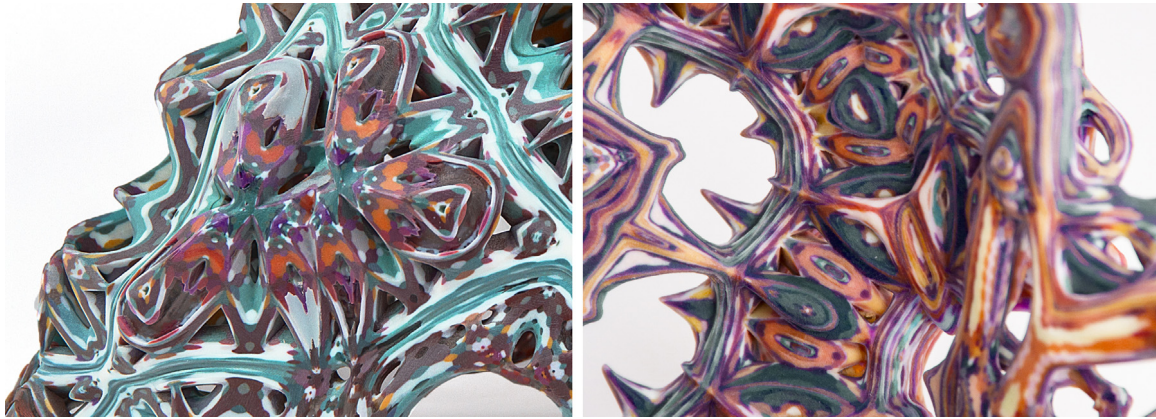


Fig. 8. Parts printed on a multi-material Stratasys J750 printer using seven base resins. The prototypes were created as part of a collection by the Mediated Matter Group in collaboration with Stratasys Ltd. for 'The New Ancient' project.

the enclosed volume. Following the identification of all internal material-compositions, the slice is dithered into n bitmaps, one for each base material, by a 3D-adaption of a process similar to Floyd–Steinberger [32] dithering. All the above can be efficiently implemented using common spatial data structures. We show two examples using different material combinations in Fig. 8, printed on Stratasys J750 using seven materials simultaneously, creating a full color and transparency printed part.

4. Conclusion

In this paper, we have presented an algorithm for the generation of complex 3-dimensional geometries incorporating heterogeneous material distribution for the creation of multi-material objects. The method presented promotes diversity in outcomes and, as such, is suitable for creative practice and design exploration. The ability to rapidly generate a wide yet diverse array of forms that are at once geometrically complex and materially heterogeneous makes it possible to design, and digitally fabricate, forms that are highly customizable. The method shown, therefore, introduces unique design opportunities that leverage, and lie at the intersection of additive manufacturing and generative design. Finally, the incorporation of material-based parameters with shape-generating methods opens up a new design space for generative modeling as well as new and exciting opportunities for creative practitioners including designers, artists and engineers. While our method generates material distributions informed by, and embedded within geometrical descriptions, future work may explore the combination of geometrical and material modeling thus offering ways in which geometry and material can simultaneously interact within a generative system.

Acknowledgments

The authors would like to acknowledge Naomi Kaempfer, Director of Art, Fashion and Design at Stratasys Ltd., and her team members – Gal Begun, Boris Belocon and Yoav Bressler – for their insights and dedication. The company's support has enabled the use of the Stratasys J750 seven material printer. We also thank Dr. James Weaver for his insights and support. The objects discussed and presented in this paper include study prototypes designed by the Mediated Matter Group for the 'New Ancient' collection by Stratasys to debut in late 2016.

Appendix A. Supplementary data

Supplementary material related to this article can be found online at <http://dx.doi.org/10.1016/j.cad.2016.09.002>.

References

- [1] Steward I, Golubitsky M. Fearful symmetry: is god a geometer? Courier Corporation; 2010.
- [2] Washburn DK, Crowe DW. Symmetry comes of age: the role of pattern in culture. University of Washington Press; 2004.
- [3] Magnus E, Arak A. Symmetry, beauty and evolution. *Nature* 1994;372(6502): 169–72.
- [4] Møller AP, Swaddle JP. Asymmetry, developmental stability and evolution. Oxford University Press; 1997.
- [5] Jacobsen T, Hofel L. Aesthetic judgments of novel graphic patterns: analyses of individual judgments. *Percept Mot Skills* 2002;95(3):755–66.
- [6] McCormack J, Dorin A, Innocent T. Generative design: a paradigm for design research. In: Proceedings of futureground. Melbourne: Design Research Society; 2004.
- [7] Bohnacker H, Gross B, Laub J, Lazzaroni C. Generative design: visualize, program, and create with processing. Princeton Architectural Press; 2012.
- [8] Nervous Systems. Cell Cycle v 3.0, <https://n-e-r-v-o-u-s.com/cellCycle/>; 2016 [accessed 03.05.16].
- [9] Autodesk. Project Shapeshifter, <http://shapeshifter.io/>; 2016 [accessed 03.05.16].
- [10] Breuninger J, Becker R, Wolf A, Rommel S, Verl A. Generative fertigung mit kunststoffen: konzeption und konstruktion für selektives lasersintern. Springer; 2012.
- [11] Omer S. PolyJet matrix™ technology a new direction in 3D printing. Rehovot: Objet Geometries Ltd.; 2009.
- [12] Oxman N, Dikovskiy D, Belocon B, Carter CW. Gemini: Engaging experiential and feature scales through multimaterial digital design and hybrid additive-subtractive fabrication. *3D Print Addit Manuf* 2014;1(3):108–14.
- [13] Stiny G. Introduction to shape and shape grammars. *Environ Plann B* 1980; 7(3):343–51.
- [14] Hsiao SW, Chen CH. A sematic and shape grammar based approach for product design. *Des Stud* 1997;18(3):275–96.
- [15] Stiny G. Ice-ray: a note on the generation of Chinese lattice designs. *Environ Plann B: Plann Des* 1977;4(1):89–98.
- [16] Heisserman L. Generative geometric design. *IEEE Comput Graph* 1994;14(2): 37–45.
- [17] Botsch M, Kobbelt L, Pauly M, Alliez P, Levy B. Polygon mesh processing. CRC Press; 2010. p. 133.
- [18] Catmull E, Clark J. Recursively generated B-spline surfaces on arbitrary topological meshes. *Comput-Aided Des* 1978;350–5.
- [19] Bærentzen JA, Gravesen J, Anton F, Aanaes H. Guide to computational geometry processing. London: Springer; 2012. p. 132.
- [20] Ervinck N. Studio Nick Ervinck, <http://www.nickervinck.com/>; 2016 [accessed 03.05.16].
- [21] Hansmeyer M. Michael Hansmeyer - Computational Architecture, <http://www.michael-hansmeyer.com/>; 2016 [accessed 03.05.16].
- [22] Shaker N, Togelius J, Nelson MJ. Procedural content generation in games: a textbook and an overview of current research. Springer; 2015.
- [23] Botsch M, Steinberger S, Bischoff S, Kobbelt L. Openmesh - a generic and efficient polygon mesh data structure. RWTH Aachen, 2002.

- [24] Konukoglu E, Glocker B, Criminisi A, Phol KM. WESD – weighted spectral distance for measuring shape dissimilarity. *IEEE Trans Pattern Anal* 2013; 35(9):2284–97.
- [25] Reuter M, Wolter FE, Peinecke N. Laplace–Beltrami spectra as ‘Shape-DNA’ of surfaces and solids. *Comput Aided Des* 2006;38(4):342–66.
- [26] Meyer M, Desbrun M, Schröder P, Barr AH. Discrete differential-geometry operators for triangulated 2-manifolds. In: *Visualization and mathematics III*. Berlin, Heidelberg: Springer; 2003. p. 35–57.
- [27] Man KF, Tang KS, Kwong S. *Genetic algorithms: concepts and designs*. Springer Science & Business Media; 2012.
- [28] Aron J. The mandelbulb: first true 3D image of famous fractal. *New Sci* 2009; 204(2736):54.
- [29] Kobbelt LP, Botsch M, Schwanecke U, Seidel HP. Feature sensitive surface extraction from volume data. In: *Proceedings of the 28th annual conference on computer graphics and interactive techniques*. 2001. p. 57–66.
- [30] Wonjoon C, Sachs EM, Patrikalakis NM, Troxel DE. A dithering algorithm for local composition control with three-dimensional printing. *Comput Aided Des* 2003;35(9):851–67.
- [31] Bader C, Kolb D, Weaver JC, Oxman N. Data-driven material modeling with functional advection for 3D printing of materially heterogeneous objects. *3D Print Addit Manuf* 2016;3(2):71–9.
- [32] Floyd RW, Steinberger L. An adaptive algorithm for spatial gray-scale. In: *Proceedings of the society of information design*. 1976.